

# We are IntechOpen, the world's leading publisher of Open Access books Built by scientists, for scientists

6,900

Open access books available

186,000

International authors and editors

200M

Downloads

Our authors are among the

154

Countries delivered to

TOP 1%

most cited scientists

12.2%

Contributors from top 500 universities



WEB OF SCIENCE™

Selection of our books indexed in the Book Citation Index  
in Web of Science™ Core Collection (BKCI)

Interested in publishing with us?  
Contact [book.department@intechopen.com](mailto:book.department@intechopen.com)

Numbers displayed above are based on latest data collected.  
For more information visit [www.intechopen.com](http://www.intechopen.com)



# Application of Simulated Annealing on the Study of Multiphase Systems

Maurice G. Politis<sup>1</sup>, Michael E. Kainourgiakis<sup>2</sup>, Eustathios S. Kikkinides<sup>1</sup>  
and Athanasios K. Stubos<sup>2</sup>

<sup>1</sup> University of Western Macedonia, Department of Engineering and Management of Energy Resources, Bakola & Sialvera Str., 50100, Kozani

<sup>2</sup> National Center for Scientific Research Demokritos, 15310 Ag. Paraskevi Attikis, Athens, Greece

## 1. Introduction

*“πάντα δὲ δοκιμάζετε, τὸ καλὸν κατέχετε, ἀπὸ παντὸς εἴδους πονηροῦ ἀπέχεσθε.”*

*“Try everything, keep the good, stay away from all form of evil.”*

(St. Paul, 1 Thessalonians 5:21-22)

The study of multiphase systems is of great importance in various fields of technological and environmental interest such as oil recovery, gas separations by adsorption, study of hazardous waste repositories and catalysis (Mohanty, 2003). In the past decade there has been considerable interest in numerical simulation studies (Baldwin et al., 1996; Torquato, 2005; Kumar et al. 2008) where an accurate representation of the complex multiphase matrix at the pore scale enables detailed studies of equilibrium and dynamic processes in these structures. Understanding the relationship between multiphase distribution at the microscale and transport properties is a general problem in applications involving multiphase systems (Kosek et al., 2005; Bruck et al., 2007). However, the direct correlation of experimental transport data to the underlying microscopic multiphase distribution is often found to be a very complicated procedure mainly because the multiphase configuration structure itself is highly complex and inadequately known. Hence, there is a strong need for a direct quantitative description of the pore-solid structure and the single or multi phase fluid distribution within this structure that should provide the basis for a reliable determination of the respective macroscopic transport properties. Such a methodology could contribute significantly to the efficient design of improved porous materials and multiphase flow processes.

Simulated Annealing has become a paradigm methodology in many areas of non-linear multiparameter global optimization. It represents a powerful and algorithmically simple solution to some of the most demanding computational task. One could summarize the method in one sentence: try all that matter, keep the best and stay away from local traps. The scope of this chapter is to demonstrate the effectiveness of SA for the realistic three-dimensional (3D) representation of the complex landscapes of multiphase systems thus enabling the simulation of disordered microstructures as they are experimentally observed in real materials.

Source: Simulated Annealing, Book edited by: Cher Ming Tan, ISBN 978-953-7619-07-7, pp. 420, February 2008, I-Tech Education and Publishing, Vienna, Austria

Disordered materials, such as glasses, liquids and random heterogeneous materials, (Torquato, 2002) have a structure that is stochastic in nature. Their microstructure defines a random field, fully characterized by n-moments of the phase-function or simplified phenomenological expressions that contain semi-empirical parameters that implicitly depend on these moments. In this context are defined the effective properties of the system that can be expressed as ensemble averages (expectations) of the moment generating probability functions. It is then natural to approximate such properties by ergodic averages through Monte Carlo simulation. The derivation of the mathematical expressions for the ensemble averages is the subject of homogenisation theory and gives the necessary formal justification for the definition of effective properties such as conductivity, permeability, elastic moduli and wetting factors.

The SA methodology will be illustrated in two applications:

1. To solve an inverse problem for a two-phase, solid-void medium, namely the 3D microstructure reconstruction from statistical descriptors based on two-dimensional (2D) cross-sections of real-world materials.
2. To determine the fluid spatial distribution in a multiphase system (pore-solid-fluid).

An inverse, ill-posed problem implies that there are many realizations of a porous medium that share the same objective function and there is no unique solution. When solving the reconstruction problem, the minimization of the objective function (system 'energy') has no physical significance and only serves as an ad hoc optimization variable. Thus, even intermediate, far from optimal, solutions represent a physically valid microstructure. This should be distinguished conceptually from finding the global minimum for the fluid distribution case that entails only the optimal solution as the one corresponding to a situation matching reality. Examples of the latter are common in many areas of Physical Chemistry where Statistical Thermodynamics formulations provide the theoretical basis for Monte Carlo simulations.

To determine the fluid spatial distribution in the three-phase system it is also necessary to decouple the effect of the solid-void interface, which is structure depended and thus requires geometrical analysis, from the effect fluid-solid and fluid-fluid interface which depend on thermodynamic and physicochemical concepts and require the application of microscopic analysis in the form of simple or complex thermodynamic rules (Kainourgiakis et al., 2002).

## 2. Optimization problem

The multiphase distribution problem can be formulated as an optimization problem, seeking to minimize the difference between the statistical properties of the generated structure and the imposed ones. Simulated annealing (SA) was originally formulated as an optimization algorithm by Kirkpatrick and coworkers (Kirkpatrick et al., 1983). They used the Metropolis algorithm to solve combinatorial problems establishing an analogy between the annealing process in solids, the behavior of systems with many degrees of freedom in thermal equilibrium at a finite temperature and the optimization problem of finding the global minimum of a multi-parameter objective function.

A randomly generated perturbation of the current system configuration is applied so that a trial configuration is obtained. Let  $E_c$  and  $E_t$  denote the energy level of the current and trial configurations, respectively. If  $E_c \geq E_t$ , then a lower energy level has been reached, the trial configuration is unconditionally accepted and becomes the current configuration. On the other hand, if  $E_c < E_t$  then the trial configuration is accepted with a probability given by  $P(\Delta E) = e^{(-\Delta E/k_B T)}$  where  $\Delta E = E_t - E_c$ ,  $k_B$  is the Boltzmann constant and  $T$  is the temperature (or an arbitrary analog of it, used only to symbolically represent the degree of randomness in the spatial distribution of the system phases). This step prevents the system from being trapped in a local lowest-energy state. After a sufficient number of iterations, the system approaches equilibrium, where the free energy reaches its minimum value. By gradually decreasing  $T$  and repeating the simulation process (using every time as initial configuration the one found as equilibrium state for the previous  $T$  value), new lower energy levels become achievable. The process is considered complete when despite the change in  $T$  the number of accepted changes in different configurations becomes lower than a pre-specified value.

The two applications that will be presented can be seen in from a very different perspective. The reconstruction of random media is an intriguing inverse problem that must be interpreted in the appropriate physical context whereas the fluid-phase distribution is a purely numerical exercise in finding the global minimum.

In trying to address the non-uniqueness problem we have proposed (Politis et al., 2008) a novel methodology that uses a simple process-based structure, matching only limited structural information with the target material, to initialize the simulated annealing and thus reduce the search-space, constraining the solution path. The stochastic / process-based hybrid method starts with a random sphere pack obtained using the ballistic deposition algorithm as the process-based step and then uses SA to minimize the least-squares error functional of the correlation functions (Kainourgiakis et al., 1999; Kainourgiakis et al., 2005).

### 3. Reconstruction of random media

The reconstruction of realizations of random media is of interest although it is possible to directly obtain, at least for some materials, high resolution ( $\sim 200\text{nm}/\text{pixel}$ ) 3D microtomography images (Spanne et al 2001; Tomutsa & Radmilovic 2003). The use of limited information from low-order correlations can offer a valuable theoretical probe to the very nature of the complex structure (Sheehan & Torquato, 2001; Torquato, 2005). Exploring all physically realizable correlation functions enables the investigation of effective properties in ad hoc reconstructed materials that suit the experimenter.

There are several techniques to statistically generate the 3D structures but broadly fall in three categories:

1. *Gaussian Random Fields*: Based on thresholding a Gaussian random field, was the first to be introduced by P. M. Adler and co-workers (Adler et al., 1990; Adler, 1992; Thovert et al., 2001). The reconstruction is based on and limited to the porosity and 2-point correlation function of the sample, measured by image analysis. The method is

- computationally very efficient but can not use additional spatial correlation functions or extended to non-Gaussian statistics.
2. *Simulated Annealing optimization*: These methods attempt to reconstruct the phase function from theoretically any number of stochastic functions that describe the sample geometry (Rintoul & Torquato, 1997; Yeong & Torquato 1998a; Yeong & Torquato 1998b; Torquato, 2002). Computationally they can be demanding if higher order statistical moments are used (e.g. chord length, lineal path or 3-point correlation).
  3. *Maximum entropy methods*: They are derived from Bayesian statistics methods first applied for inverse problems is signal processing. Microstructures are assumed to be samples from a governing probability distribution function (PDF) which is computed from the limited available statistical descriptors (correlation functions) using maximum entropy theory (Sankaran & Zabaras, 2006).

An alternative method to obtain the microstructure is to simulate the physical (thermo-mechanical) process that they result from, in effect recreating the material synthesis history. This is an extremely complex and computationally very expensive process but still viable in small domains (Bakke & Oren, 1997; Bryant & Blunt, 2004).

Effective reconstruction of random two-phase heterogeneous media can be realized from statistical descriptors, namely n-point correlation functions, obtained from digitized images of a material. The n-point correlation function is a measure of the probability of finding n-points (in a specified geometrical arrangement) all lying in the region of space occupied by one constituent of a two-phase material. For example the one-point correlation function is the probability that any point lies in a specific phase (either pore or solid phase). Thus if we define the phase function of a porous material as follows (Berryman, 1985; Torquato, 2002):

$$Z(\mathbf{x}) = \begin{cases} 1, & \text{if } \mathbf{x} \text{ is in phase 1 (pore)} \\ 0, & \text{if } \mathbf{x} \text{ is in phase 2 (solid)} \end{cases} \quad (1)$$

If the medium is statistically homogeneous, then the probability functions are translationally invariant in space and depend only on the spatial separation between the points. Then it follows that the 1-point correlation function is by definition equal to the porosity:

$$\varepsilon = S_1(\mathbf{u}) = \langle Z(\mathbf{x}) \rangle \quad (2)$$

The angular brackets denote an ensemble average. Accordingly, the 2-point correlation function is the probability that two points at a specified distance can be found both in the same phase of the material:

$$S_2(\mathbf{u}) = \langle Z(\mathbf{x}) \rangle \langle Z(\mathbf{x} + \mathbf{u}) \rangle \quad (3)$$

In general,

$$S_n(\mathbf{x}_1, \dots, \mathbf{x}_n) = \left\langle \prod_{i=1}^n Z(\mathbf{x}_i) \right\rangle \quad (4)$$

An additional simplification can be made if the medium is statistically isotropic. For an isotropic medium,  $S_2(u)$  becomes one-dimensional as it is only a function of  $u = |\mathbf{u}|$ . It is often preferable to work with the 2-point auto-correlation function  $R_z(\mathbf{u})$  which is a normalized version of  $S_2(u)$ :

$$R_z(\mathbf{u}) = \frac{\langle (Z(\mathbf{x}) - \varepsilon) \cdot (Z(\mathbf{x} + \mathbf{u}) - \varepsilon) \rangle}{\varepsilon - \varepsilon^2} \quad (5)$$

Note that if we reverse the phase function in order to calculate the n-point correlation functions for the solid phase we observe that  $R_z(u)$  remains exactly the same; simply change  $Z$  to  $1-Z$ , and  $\varepsilon$  to  $1-\varepsilon$  everywhere in eq. (5). For a statistically homogenous and spatially ergodic medium, the spatial average is equivalent to the ensemble average and thus we can define and compute the average quantities of the medium.

Based on the work of Debye (Debye et al., 1957), the 2-point correlation function can be related to the interface area per unit volume of the material. The specific internal surface area per unit volume ( $S_v$ ) can be determined from the slope of  $R_z(\mathbf{u})$  at  $u=0$  using eq. (6), adjusted for a digitized 3D medium (Jiao et al., 2007):

$$S_v = -6\varepsilon(1 - \varepsilon) \left. \frac{dR}{du} \right|_{u=0} \quad (6)$$

$S_v$  can also be directly calculated from the reconstructed binary realization by counting the pixels at the void-solid interface.

A reconstruction of a porous medium in three dimensions should reproduce the same statistical correlation properties as those obtained from the two-dimensional image and defined by the n-moments of the phase function. In this work we only match the trivial one-point correlation function, the porosity  $\varepsilon$ , and the two-point auto-correlation function which contain information about the phase size, orientation and surface area. Other important descriptors that can be used are the lineal path function, the chord length function and the three-point correlation function (Torquato & Lee, 1990; Torquato, 2002). Reconstructing a material using limited microstructural information is an inverse, ill-posed problem, i.e. there are many realizations of a porous medium that share same the porosity and two-point correlation function. The choice to use only two functions can thus sometimes be inadequate to reproduce the material microstructure. Matching higher order correlation functions should also be considered (Kainourgiakis et al., 2000) but it is computationally much more expensive for the realization of sufficiently large 3D domains.

### 3.1 SA and process-based hybrid reconstruction of porous media

In the typical SA method we start from a completely random initial distribution of the phase function in space. In the proposed hybrid method we start with an initial configuration

provided by the output of a process-based method such as the described ballistic deposition of equal spheres. The porosity of the initial structure must be equal with that of the original structure (usually the source image).

The next step is to define the Energy,  $E$ , of our system. In this case  $E$  is the sum of squared differences between experimental correlation functions obtained from the SEM micrographs, and those calculated from the 3D generated structure.

$$E = \sum_i \sum_j [S_i(u_j) - S_i^{\text{exp}}(u_j)]^2 \quad (7)$$

index  $i$  corresponds to the degree of the correlation function, and index  $j$ , corresponds to the digitized distance  $u$ . If only the two-point correlation function interests us, then  $i = 2$  and the first summation is dropped out from eq. (7). Note that in the above algorithm, the one-point correlation function (porosity) is always identical to the experimental by construction. The SA algorithm for the reconstruction problem has as follows:

1. Create a candidate 3D image using random packing of spheres with a volume fraction equal to the target microstructure. Adjust the porosity, if necessary, using Grain Consolidation to match that of the target medium. Calculate the initial energy  $E_c$ .
2. A new trial state is obtained by interchanging (swapping) two arbitrarily selected pixels of different phases. This way the initial porosity of the structure is always preserved. Accordingly the energy of the trial state  $E_t$  is determined through eq. (7).
3. If  $E_c \geq E_t$ , the trial configuration is unconditionally accepted, and becomes the current configuration. On the other hand, if  $E_c < E_t$  then the trial configuration is accepted with a probability  $P(\Delta E) = e^{-\Delta E/k_B T}$ .
4. Steps 2, 3 are repeated at the same temperature  $T$ .
5. Decrease temperature by a very slow rate and repeat steps 2-4.
6. The process terminates when the successful exchanges become less than a specified number per iteration.

The process is terminated when the number of accepted changes in different configurations becomes lower than a pre-specified value. The most time-consuming step in the SA method is the determination of  $E$  through the repeated calculation of the correlation function(s) at each pixel interchange. Nevertheless, this calculation can be improved considerably by observing that once  $S_2(\mathbf{u})$  of the initial structure is calculated there is no need to fully sample all intermediate (trial) structures since any change in the correlation function(s) will be only due to the change along the x-, y- and z- direction that cross each altered pixel (two pixels at each swapping). This change in  $S_2$  can be simply evaluated by invoking the sampling procedure only along those rows, columns and heights crossing the altered pixels, adjusting appropriately the initially stored  $S_2(\mathbf{u})$ .

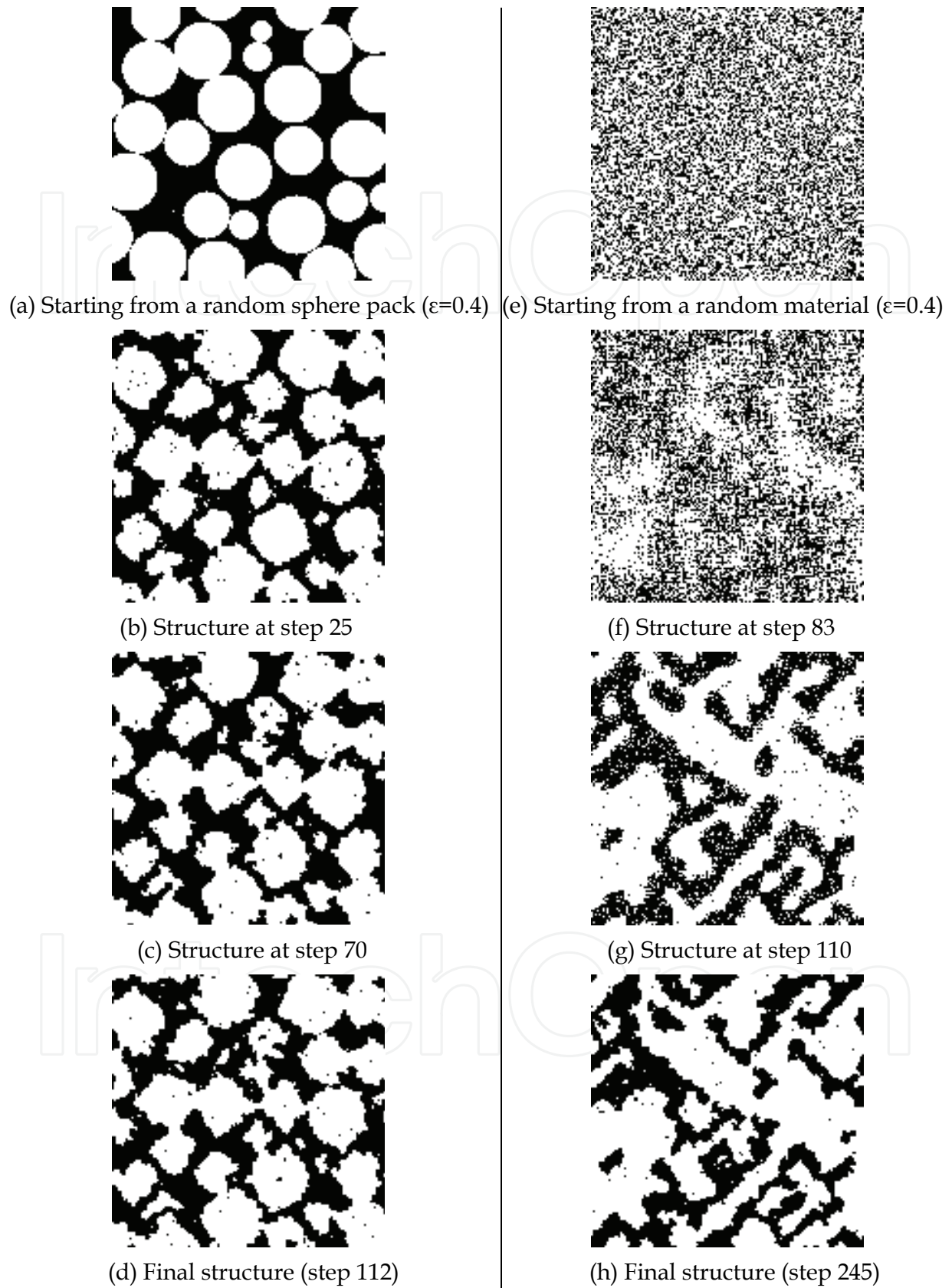


Figure 1. Progress of the evolving microstructure at specific SA instances. The material shown is the sintered SiC case ( $\epsilon = 0.4$ ). Image size is  $140 \times 140$  pixels. (solid is shown white)

An important parameter in the SA algorithm is the initial temperature  $T_0$ , particularly if the original structure is not truly random but has some noticeable degree of correlation as it is the case of starting with a random sphere pack as input. If  $T_0$  is too low then the algorithm is quite immobile, not many swaps are accepted and the initial structure is quite close to the final structure. On the other hand, if  $T_0$  is not too low, the algorithm becomes quite mobile, swaps are accepted more easily and the initial structure is not close to the final structure.

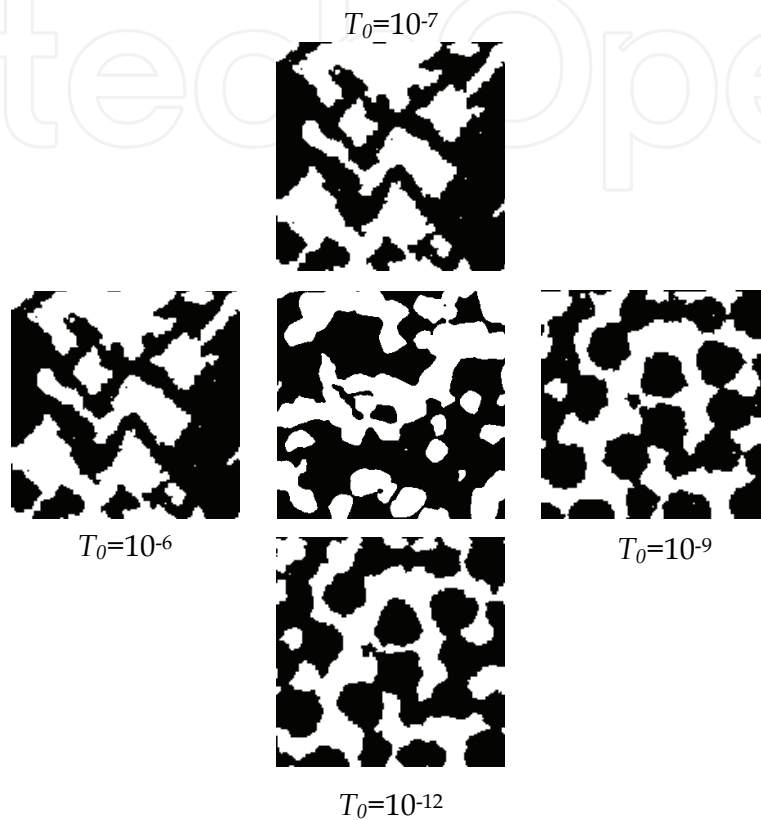


Figure 2. The effect of initial SA temperature, the target structure is in the middle, porosity is  $\sim 42\%$  and solid-space is shown black.

#### 4. Determination of the spatial fluid distribution

To determine the multi-phase fluid distribution in porous material, the porous structure is represented by a set of cubic voxels of length  $\ell$ . Each voxel is labeled by an integer that corresponds to its phase. The solid phase is labeled as 0 while the fluid phases as  $1, 2, 3, \dots, n$ . The saturation of the phase  $i$ , denoted as  $S_i$ , is the volume fraction of the pore space occupied by the phase  $i$ . The distribution of the  $n$  fluid phases in the pore space is determined assuming that the total interfacial free energy,  $G_s$ , is minimal. The function  $G_s$  can be evaluated by:

$$G_s = \sum_{i=0}^{n-1} \sum_{j>i}^n A_{ij} \sigma_{ij} \quad (8)$$

where  $A_{ij}$  is the elementary  $ij$  interfacial area and  $\sigma_{ij}$  the interfacial free energy per unit area of  $ij$  interface. The interfacial free energies obey Young's equation and consequently the following set of  $\frac{n(n-1)}{2}$  equations is satisfied (van Kats & Egberts, 1998):

$$\sigma_{0i} = \sigma_{0j} + \sigma_{ij} \cos \theta_{ij} \quad (9)$$

where  $\theta_{ij}$  is the contact angle that the  $ij$  interface forms with the solid surface,  $i \neq 0$ ,  $j \neq 0$  and  $i < j$ . The determination of the spatial distribution of fluid phases that corresponds to the minimum  $G_s$  is achieved by exploring all possible configurations. In practice this is impossible since the number of configurations is extremely high and consequently, the optimal one must be determined by importance-sampling procedures. When only two fluid phases are present, the simplest and rather inefficient heuristic technique that can be used is the following: A specified number of voxels, in random positions of the pore space, are marked as sites occupied by phase 1 while the rest are marked as belonging to phase 2. The number of sites occupied by each fluid phase corresponds to a desired fraction of pore space occupied by that phase (saturation). Then two randomly selected sites occupied by different fluid phases exchange their positions. This change results in a variation of  $G_s$  by an amount  $\Delta G_s$ . To minimize  $G_s$ , one can accept every phase exchange trial with  $\Delta G_s \leq 0$  and reject those where  $\Delta G_s > 0$ . However, due to the complicated  $G_s$  landscape with respect to the spatial distribution of the fluid phases, local minima are present and when the system reaches one of them no escape is possible (Knight et al., 1990).

The SA algorithm is used for the minimization of the multidimensional functions as originally adapted for a similar problem by Knight et al. (1990). Now, the new configuration that is generated by the phase exchange of random voxels is accepted with a probability given by:

$$p = \min \left( 1, e^{-\Delta G_s / G_{ref}} \right) \quad (10)$$

where  $G_{ref}$  is an analog of the  $k_B T$  parameter in the Metropolis algorithm and  $k_B$ ,  $T$  are the Boltzmann constant and the ambient temperature respectively. After a sufficient number of iterations (usually ten-times the number of the pixels occupied by the fluid phases) and for a specific  $G_{ref}$  value, the system approaches the equilibrium state. By gradually decreasing  $G_{ref}$ , according to a specified "cooling schedule" and repeating the simulation process, using every time as initial configuration the one found as equilibrium state for the previous  $G_{ref}$  value, new lower energy levels of  $G_s$  become achievable. The process is considered complete when despite the change in  $G_{ref}$ , the number of accepted changes in different configurations becomes lower than a pre-specified value (typically when the ratio of the number of acceptable moves to the total number of trials becomes lower than  $10^{-5}$ ). The above technique can be generalized for  $n$  fluid phases distributed in the pore space. Each voxel of the pore space is randomly characterized by an integer,  $1, 2, \dots, n$ , that corresponds to one of the existing fluid phases. The number of voxels that are occupied by

each phase satisfies a predefined saturation of the specific phase,  $S_i$ . Then, two voxels belonging to fluid phases are randomly selected, their phases are exchanged and the swap is accepted with probability according to eq. (10). This procedure is termed procedure (A). To employ a more efficient minimization strategy, termed procedure B,  $n$  voxels occupied by different fluid phases are randomly selected at each minimization step. Then,  $n(n-1)/2$  voxel-phase interchanges are performed. For the case of three fluid phases, the trial swaps are 1-2, 1-3 and 2-3. Each trial swap is accompanied by a variation of  $G_s$  by  $\Delta G_{s,ij}$ , where  $i < j$ . If at least one  $\Delta G_{s,ij} < 0$ , the trial swap with the minimum  $\Delta G_{s,ij}$  is accepted. In the opposite case, where every  $\Delta G_{s,ij} > 0$ , the swap  $ij$  is accepted with probability  $p_{ij}$  defined as:

$$p_{ij} = \frac{e^{-\Delta G_{s,ij}/G_{ref}}}{n(n-1)/2} \quad (11)$$

Note that since  $e^{-\Delta G_{s,ij}/G_{ref}}$  then  $\sum_{i=1}^{n-1} \sum_{j>i}^n p_{ij} \leq 1$  and therefore the system remains unchanged

with probability  $q = 1 - \sum_{i=1}^{n-1} \sum_{j>i}^n p_{ij}$ . After a sufficient number of iterations,  $G_{ref}$  is gradually

decreased and the system approaches the lowest energy configuration. It must be noticed that for  $n = 2$  the acceptance rule described by eq. (10) is recovered.

The simple case of a single pore with square cross section containing three fluid phases is selected to start with. The size of the pore is  $50 \times 50 \times 100$  and the saturation of each phase is equal to  $1/3$ . The corresponding interfacial free energies in arbitrary energy units per unit area (square voxel length) are  $\sigma_{01} = 3000$ ,  $\sigma_{02} = 2500$ ,  $\sigma_{03} = 1200$ ,  $\sigma_{12} = 500$ ,  $\sigma_{13} = 1800$ ,  $\sigma_{23} = 1200$  and consequently  $\theta_{12} = \theta_{13} = \theta_{23} = 0$ . Thus, the labels 1,2,3 correspond to the non-wetting, intermediate wetting and wetting phases respectively. The "cooling schedule", the initial choice of  $G_{ref}$  and the minimization strategy are determined with the help of this simple pore geometry. The results obtained are used for the determination of the phase distribution in more complicated porous domains. The "cooling schedule" applied is:

$$G_{ref} = f^N G_{ref,0} \quad (12)$$

where  $f$  is a tunable parameter obeying  $0 < f < 1$ ,  $N$  is the number of iterations for a given  $G_{ref}$  and  $G_{ref,0}$  is the initial choice of  $G_{ref}$ . A "cooling schedule" of this form is used by Knight et al. (1990) and has the advantage that during the annealing process the variation of  $G_{ref}$  decreases, allowing for better resolution as the system approaches the optimal configuration. The value of the parameter  $f$  plays a dominant role in the simulation. Small  $f$  values decrease  $G_{ref}$  quickly resulting in fast simulations, however the risk of local minima trapping is high in that case. Contrarily, when  $f$  approaches unity the simulation becomes lengthy in time but the system escapes more efficiently from metastable

configurations. Figure 3 illustrates the distribution of the fluid phases obtained for different  $f$  values. It is observed that for  $f < 0.999$  the simulation produces final configurations where, although some clusters are present, the phases are rather randomly mixed. As  $f$  increases, physically sound configurations appear. The wetting phase (blue) is located in contact with the solid walls, the non wetting phase (red) forms a cylinder-like cluster at the center of the pore while the intermediate wetting phase (green) fills the space between the wetting and the non-wetting ones. In Fig. 4 the minimum total interfacial energy,  $G_{s,min}$ , is plotted against  $f$ . It is noteworthy that the total interfacial energy values are considerably close to each other, compared with their absolute values, although the distribution of the fluid phases in Fig. 3 is undoubtedly different. This indicates that the minimization procedure must be handled with care. In the present work, in order to achieve as accurately as possible the configuration with minimum interfacial energy,  $f = 0.999$  is used.

At the beginning of the simulation, another important issue that must be considered is the initial choice of  $G_{ref}$ . The value of  $G_{ref,0}$  must be large enough, approximately 30-times the highest  $\sigma_{ij}$  value, in order to ensure that the system is initially in a “molten” state and not trapped in a local minimum. When  $G_{ref,0}$  is not large enough the system cannot approach the optimal distribution.

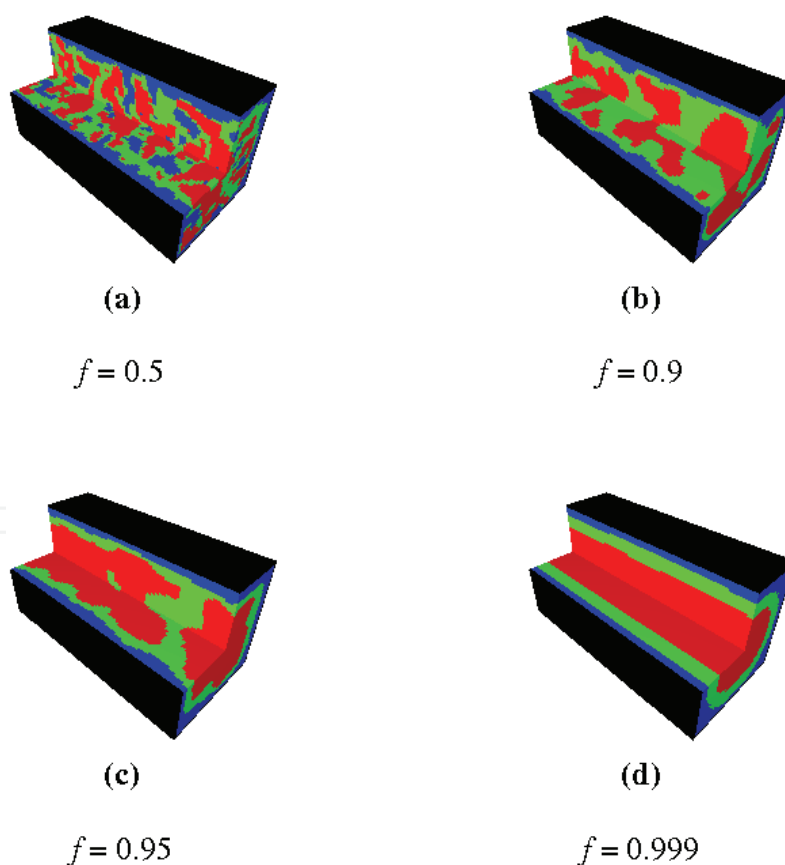


Figure 3. Phase distribution in a rectangular pore for different  $f$  values when three fluid phases are present. Blue color: wetting phase, green color: intermediate wetting phase, red color: non wetting phase. The saturation of each phase is  $1/3$ .

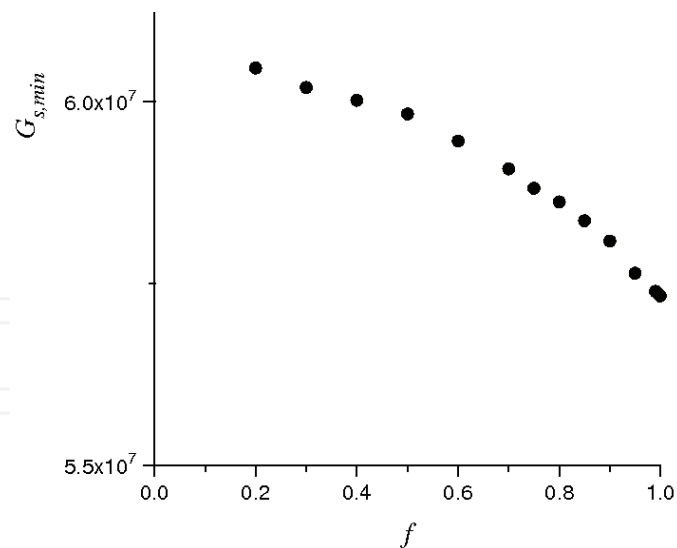


Figure 4. Minimum interfacial energy vsf for rectangular pore containing three fluid phases. The saturation of each phase is  $1/3$  and the initial choice of  $G_{ref}$  is  $10^5$ .

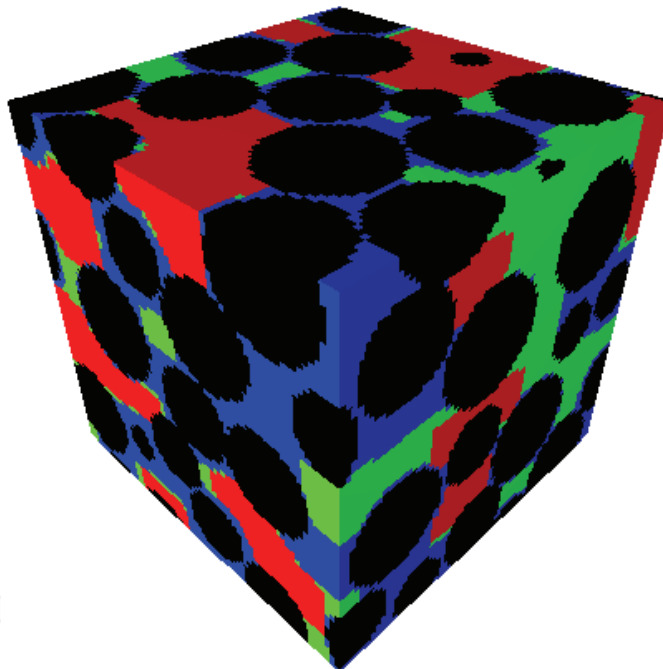


Figure 5. Phase distribution in a random sphere packing when three fluid phases are present. Blue color: wetting phase, green color: intermediate wetting phase, red color: non wetting phase. The saturation of each phase is  $1/3$ .

## 5. Evaluation of the SA method for the reconstruction problem

To demonstrate the proposed method (Politis et al., 2008) we have chosen to calculate the air permeability of a sintered silicon carbide (SiC) ceramic characterized in-house and the Ni-YSZ anode cermet of a solid oxide fuel cell (SOFC) found in the literature (Lee et al, 2004). The backscatter electron SEM micrographs of both materials were digitized using standard image processing techniques (Ioannidis et al., 1996). Both materials are consolidated,

produced using a fine powder substrate that is sintered at an elevated temperature. In total we have generated two realizations for each material: one using the hybrid method and starting from the porosity-matching random sphere pack and one by using the SA algorithm with a random initial structure.

### 5.1 Constructing the microstructure

The reconstructed material domains are three-dimensionally periodic with a simulation volume of  $140^3$  pixels and a porosity of  $\sim 40\%$ . The mean pore size though differs by almost an order of magnitude:  $10.2 \mu\text{m}$  for SiC and  $0.9 \mu\text{m}$  for Ni-YSZ. In Fig. 6, we plot the two-point auto-correlation function for the test-target materials, as obtained from the digitized SEM images. The corresponding two-point correlation function of the reconstructed structure it is not shown as it is an exact match. This is expected because it is the only optimization target for the SA algorithm. If more additional correlation functions are added then the match becomes non-trivial. We can noticed that for SiC the  $R_z(u)$  drops practically to zero after  $\sim 16 \mu\text{m}$ , meaning that there is no correlation after this length. Similarly, for Ni-YSZ, there is no correlation after  $\sim 4 \mu\text{m}$ . The domains used in the computations are equal to  $140^3$  pixels for both structures, resulting in spatial dimensions of  $200 \mu\text{m}^3$  for SiC and  $21.5 \mu\text{m}^3$  for Ni-YSZ.

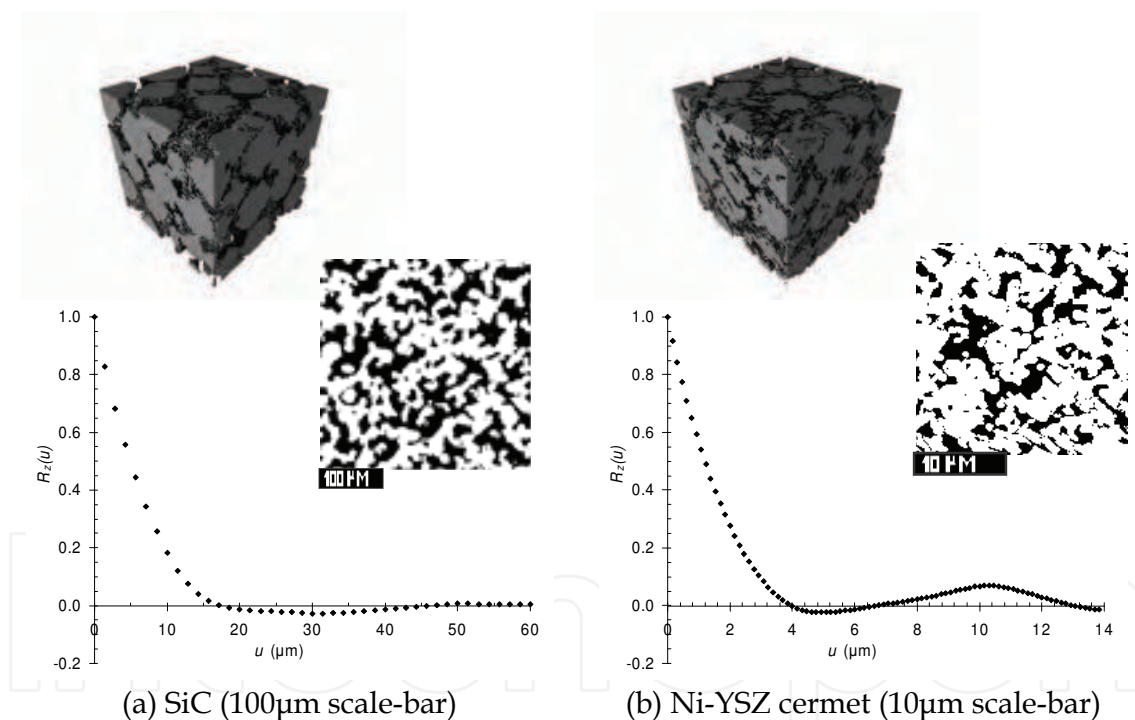


Figure 6. Binarized SEM image, 2-point autocorrelation function and 3D hybrid reconstruction realization with a volume of  $100^3$  pixels that represent  $142.8 \mu\text{m}^3$  for the SiC and  $15.4 \mu\text{m}^3$  for the Ni-YSZ (pore space is transparent for clarity). The Ni-YSZ porosity is 0.40 with an image size of  $154 \times 154$  pixels (pixel length  $\sim 0.154 \mu\text{m}$ ). The SiC porosity is 0.40 with an image size of  $235 \times 235$  (pixel length  $\sim 1.428 \mu\text{m}$ ).

### 5.2 Absolute permeability calculations

The absolute permeability of the porous material gives a measure of the resistance of the porous medium in the viscous incompressible fluid flow through its pore space. In a

representative macroscopic element of homogeneous and isotropic porous material the superficial velocity,  $\langle v_s \rangle$ , of a viscous fluid is described by Darcy's law

$$\langle v_s \rangle = -\frac{k}{\eta} \cdot \overline{\nabla p} \quad (13)$$

where  $\overline{\nabla p}$  is a prescribed pressure gradient,  $k$  is the permeability coefficient, which depends on the spatial distribution of solid and void phase and  $\eta$  is the fluid viscosity.

The calculation of the permeability coefficient  $k$ , requires the determination of the flow field at the microscale at creeping flow conditions, described by the Stokes equation coupled with the continuity equation:

$$\eta \nabla^2 \mathbf{v} = \nabla p \quad (14a)$$

$$\nabla \cdot \mathbf{v} = 0 \quad (14b)$$

where  $\mathbf{v}$  and  $p$  are the local fluid velocity vector and the pressure, respectively. The boundary conditions are no-slip of the fluid at the solid-void interface and periodicity.

The numerical method employed in this work is a finite difference scheme, used previously in similar studies (Quiblier, 1984; Adler et al., 1990; Coelho, 1997; Liang et al., 2000). A staggered marker-and-cell mesh is used, with the pressure defined at the centre of the cell, and the velocity components defined along the corresponding surface boundaries of the rectangular cell. A successive overrelaxation method is used to solve for the microscopic velocity field. To cope with the numerical instabilities caused by the continuity equation, an artificial compressibility technique has been employed (Roache, 1982). In this fashion, the steady state problem is replaced by an unsteady one, which converges to the incompressible steady state solution at sufficiently long time. Convergence was achieved when the calculated flow rate values fluctuated less than 1% across the various cross-sections of the medium (Kikkinides & Burganos, 1999).

The results for the permeability of two different porous materials, using air as the flowing fluid, are summarized in Table 1.

	Air Permeability (m <sup>2</sup> )		
	Experiment	Simulation	
		Hybrid method	SA only
Ni-YSZ cermet	6.0×10 <sup>-15</sup>	5.67×10 <sup>-15</sup>	4.00×10 <sup>-15</sup>
Sintered SiC	9.4×10 <sup>-13</sup>	1.07×10 <sup>-12</sup>	8.12×10 <sup>-13</sup>

Table 1: Numerically calculated and experimentally measured permeability values for the Ni-YSZ cermet and sintered SiC.

It is evident that the permeability results obtained from the hybrid reconstruction method in excellent agreement for Ni-YSZ (within 5%) and very close for SiC (within 13%). The permeability of the SiC that resulted using the SA alone, overestimates the experimental value as much as the hybrid method underestimates it. For Ni-YSZ the error is much more pronounced (~33%) when using SA alone. The hybrid algorithm requires less than half the processing steps of the purely SA approach (see Fig. 1) resulting in a significant speed-up of the computations.

## 6. Evaluation of the SA method for the multiphase distribution problem

The assessment of the validity of the generated multiphase distributions in a pore structure is achieved by the measurement of the relative permeability of the porous material when two or more fluids are present. A significant simplification in the calculation of this property is to consider that only one fluid is flowing each time, the rest of the fluid(s) being immobile and simply treated as additional “solid” phase in the pore structure. In such a case one can still use the methodology outlined above for the determination of the absolute permeability treating the immobile fluid(s) as an expansion of the solid phase. This procedure can be performed sequentially for each fluid in order to get the relative permeability for each fluid in the multiphase configuration (Kainourgiakis et al. 2003; Galani et al, 2007).

### 6.1 Relative permeability calculations

The effective permeability for fluid  $i$ ,  $k_{e,i}$ , which depends on the spatial distribution of solid and fluid phases, is calculated again through Darcy's law:

$$\langle v_{s,i} \rangle = -\frac{k_{e,i}}{\eta_i} \cdot \overline{\nabla p} \quad (15)$$

Where  $\langle v_{s,i} \rangle$  is the superficial velocity of a viscous fluid in a sample of the homogeneous and isotropic porous medium and  $\eta_i$  is the fluid viscosity. Then the relative permeability for fluid  $i$ ,  $k_{R,i}$ , is defined by dividing the effective permeability,  $k_{e,i}$ , with the absolute permeability,  $k$ , measured in the absence of other fluids:

$$k_{R,i} = \frac{k_{e,i}}{k} \quad (16)$$

It is evident that  $k_{R,i}$  is a non-dimensional parameter.

Galani et al (2007) calculate the relative permeabilities of two and three phase fluid distributions for mono-dispersed random sphere packs when only one fluid phase is moving with low flow rate while the other fluid phase(s) are immobile and considered as an “expansion” of the solid phase. The results for the case of a two-phase fluid system of a wetting and non-wetting fluid are given in Fig. 7 and 8.

Fig. 7 presents relative permeability as a function of the effective saturation of the wetting phase (phase 2),  $S_{e,2} = (S_2 - S_{im,2}) / (1 - S_{im,2})$ , where  $S_{im,2}$  is the residual or immobile saturation of phase 2 when the non-wetting phase (phase 1) is stagnant while the wetting phase (phase 2) is flowing. Residual saturation is the amount of a fluid (e.g. oil) that remains in a porous material after the displacement of this fluid from another immiscible fluid (e.g. water) which penetrates the porous medium. The remaining fluid is stagnant and may form scattered clusters instead of a continuous phase. Fig. 7 also presents the corresponding experimental results that were obtained by Stubos (1990) for steel particle beads of porosity 0.4, as well as semi-empirical correlations from Levec (1986). In the present work, the residual saturation value,  $S_{im,2}$ , is set equal to 0.25, just as it was measured by Stubos (1990).

In all cases the computed relative permeability curves in very good agreement with the experiments in the whole spectrum of the effective saturation of the wetting phase,  $S_{e,2}$ .

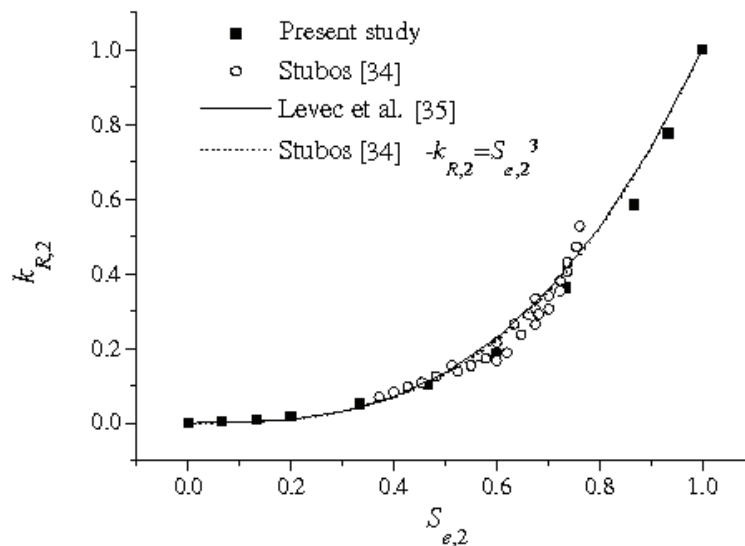


Fig. 7. Relative permeability of the wetting phase vs. the effective saturation of that phase,  $S_{e,2}$ , for the random packing of non-overlapping spheres of porosity 0.41.

Fig. 8 presents relative permeability as a function of the effective saturation of the non-wetting phase (phase 1),  $S_{e,1} = (S_1 - S_{im,1}) / (1 - S_{im,1})$ , when the wetting phase (phase 2) is

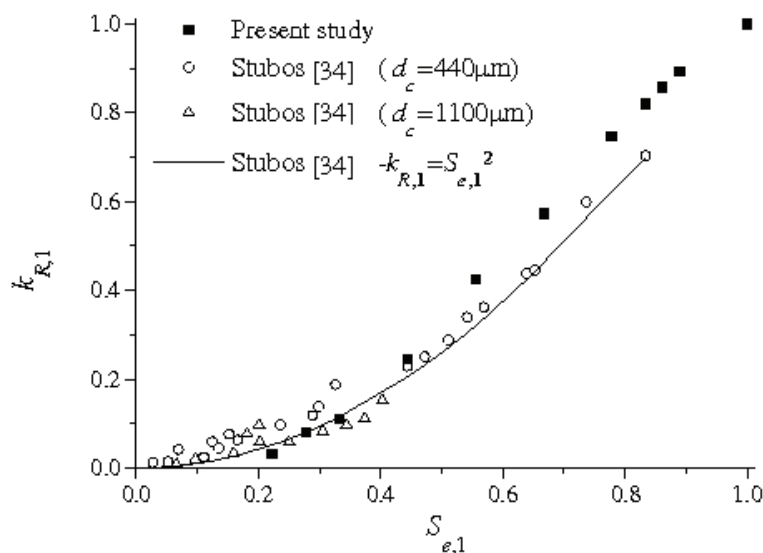


Fig. 8. Relative permeability of the non-wetting phase vs. the effective saturation of that phase,  $S_{e,1}$ , for the random packing of non-overlapping spheres of porosity 0.41.

stagnant while the non-wetting phase is flowing. The corresponding relative permeability experimental data that are used for comparison purpose have been obtained for low flow rates of the non-wetting phase. Fig. 8 also presents the corresponding experimental results

that have been obtained by Stubos (1990) for steel particle beads of porosity 0.4, for two different values of equivalent diameters,  $d_c$  and also those of the correlated function  $k_{R,1} = S_{e,1}^2$ . In the present work, the residual saturation value,  $S_{im,1}$ , was set equal to 0.12, as it was measured by Stubos (1990). The observed differences between the results of the present work and the corresponding experimental ones are again relatively small and can be explained by potential deviations between the calculated and the experimental fluid-phase distribution.

## 7. Summary

The SA method was applied to the study of multiphase, disordered systems. Determining the phase distribution in the microstructure is of fundamental importance in making a connection with their effective properties that ultimately provides a tool to design optimized and tailor-made materials. SA was shown to provide a flexible and simple to implement methodology. Two conceptually distinct problem classes were used to illustrate the method: 1) an inverse problem, the 3D microstructure reconstruction from statistical descriptors (correlation functions) extracted from standard microscopic imaging methods (e.g. SEM/TEM) and 2) finding the global optimum corresponding to the minimum energy configuration in a multiphase system (pore-solid-fluid).

In solving the reconstruction problem there are many realizations of a porous medium that satisfy the minimization of the objective function that constitutes a functional of statistical descriptors with no physical significance per se. We have proposed a novel, hybrid methodology using a defined initial structure that attempts to incorporate the natural synthesis history of the material and thus address the non-uniqueness of solution issues in the inverse problem. The method was implemented with a random sphere pack obtained using ballistic deposition as the process-based step and then matched the porosity and pair correlation function of the material with SA.

For the multiphase system, tracing the minimum of the total free interfacial energy with SA is directly equivalent with the thermodynamic distribution of the fluid phases in the pore space. The optimum configuration for a given degree of phase partitioning is derived assuming that in equilibrium the total interfacial free energy reaches a global minimum value.

The procedure has been validated by the determination of the absolute and relative permeability in the multiphase system. The agreement of the results with pertinent literature data reinforces the validity of the proposed techniques.

## 8. References

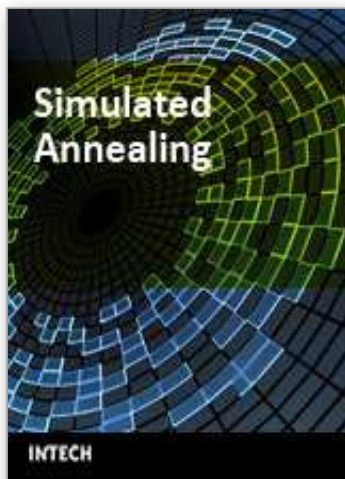
- Adler, P.M., Jacquin, C.G. & Quiblier, J.A. (1990), "Flow in simulated porous media", *International Journal of Multiphase Flow*, vol. 16, no. 4, pp. 691-712.
- Adler, P.M. 1992, *Porous Media: Geometry and Transports*, . Butterworth-Heinemann, Boston, 1992
- Bakke, S. & Øren, P.-. (1997), "3-D pore-scale modelling of sandstones and flow simulations in the pore networks", *SPE Journal*, vol. 2, no. 2, pp. 136-149.

- Baldwin, C.A., Sederman, A.J., Mantle, M.D., Alexander, P. & Gladden, L.F. 1996, "Determination and characterization of the structure of a pore space from 3D volume images", *Journal of Colloid and Interface Science*, vol. 181, no. 1, pp. 79-92.
- Berryman, J.G. (1985), "Measurement of spatial correlation functions using image processing techniques", *Journal of Applied Physics*, vol. 57, no. 7, pp. 2374-2384.
- Bruck, H.A., Gilat, R., Aboudi, J. & Gershon, A.L. (2007), "A new approach for optimizing the mechanical behavior of porous microstructures for porous materials by design", *Modelling and Simulation in Materials Science and Engineering*, vol. 15, no. 6, pp. 653-674.
- Bryant, S. & Blunt, M. (1992), "Prediction of relative permeability in simple porous media", *Physical Review A*, vol. 46, no. 4, pp. 2004-2011.
- Coelho, D., Thovert, J.-. & Adler, P.M. (1997), "Geometrical and transport properties of random packings of spheres and aspherical particles", *Physical Review E*, vol. 55, no. 2, pp. 1959-1978.
- Debye, P., Anderson Jr., H.R. & Brumberger, H. (1957), "Scattering by an inhomogeneous solid. II. the correlation function and its application", *Journal of Applied Physics*, vol. 28, no. 6, pp. 679-683.
- Galani, A.N., Kainourgiakis, M.E., Papadimitriou, N.I., Papaioannou, A.T. & Stubos, A.K. (2007), "Investigation of transport phenomena in porous structures containing three fluid phases", *Colloids and Surfaces A: Physicochemical and Engineering Aspects*, vol. 300, no. 1-2 SPEC. ISS., pp. 169-179.
- Jiao, Y., Stillinger, F.H. & Torquato, S. (2007), "Modeling heterogeneous materials via two-point correlation functions: Basic principles", *Physical Review E - Statistical, Nonlinear, and Soft Matter Physics*, vol. 76, no. 3.
- Ioannidis, M.A., Kwiecien, M.J. & Chatzis, I. (1996), "Statistical analysis of the porous microstructure as a method for estimating reservoir permeability", *Journal of Petroleum Science and Engineering*, vol. 16, no. 4, pp. 251-261.
- Kainourgiakis, M.E., Kikkinides, E.S., Galani, A., Charalambopoulou, G.C. & Stubos, A.K. (2005), "Digitally reconstructed porous media: Transport and sorption properties", *Transport in Porous Media*, vol. 58, no. 1-2, pp. 43-62.
- Kainourgiakis, M.E., Kikkinides, E.S., Charalambopoulou, G.C. & Stubos, A.K. (2003), "Simulated annealing as a method for the determination of the spatial distribution of a condensable adsorbate in mesoporous materials", *Langmuir*, vol. 19, no. 8, pp. 3333-3337.
- Kainourgiakis, M.E., Kikkinides, E.S. & Stubos, A.K. (2002), "Diffusion and flow in porous domains constructed using process-based and stochastic techniques", *Journal of Porous Materials*, vol. 9, no. 2, pp. 141-154.
- Kainourgiakis, M.E., Kikkinides, E.S., Steriotis, T.A., Stubos, A.K., Tzevelekos, K.P. & Kanellopoulos, N.K. (2000), "Structural and transport properties of alumina porous membranes from process-based and statistical reconstruction techniques", *Journal of Colloid and Interface Science*, vol. 231, no. 1, pp. 158-167.
- Kainourgiakis, M.E., Kikkinides, E.S., Stubos, A.K. & Kanellopoulos, N.K. (1999), "Simulation of self-diffusion of point-like and finite-size tracers in stochastically reconstructed Vycor porous glasses", *Journal of Chemical Physics*, vol. 111, no. 6, pp. 2735-2743.

- Kikkinides, E.S. & Burganos, V.N. (1999), "Structural and flow properties of binary media generated by fractional Brownian motion models", *Physical Review E*, vol. 59, no. 6, pp. 7185-7194.
- Kirkpatrick, S., Gelatt Jr., C.D. & Vecchi, M.P. (1983), "Optimization by simulated annealing", *Science*, vol. 220, no. 4598, pp. 671-680.
- Kosek, J., Stepanek, F. & Marek, M. (2005), "Modeling of transport and transformation processes in porous and multiphase bodies", *Advances in Chemical Engineering*, vol. 30, pp. 137-203.
- Knight, R., Chapman, A. & Knoll, M. (1990), "Numerical modeling of microscopic fluid distribution in porous media", *Journal of Applied Physics*, vol. 68, no. 3, pp. 994-1001.
- Kumar, N.C., Matouš, K. & Geubelle, P.H. (2008), "Reconstruction of periodic unit cells of multimodal random particulate composites using genetic algorithms", *Computational Materials Science*, vol. 42, no. 2, pp. 352-367.
- Liang, Z., Ioannidis, M.A. & Chatzis, I. 2000, "Permeability and electrical conductivity of porous media from 3D stochastic replicas of the microstructure", *Chemical Engineering Science*, vol. 55, no. 22, pp. 5247-5262.
- Lee, D.-., Lee, J.-., Kim, J., Lee, H.-. & Song, H.S. (2004), "Tuning of the microstructure and electrical properties of SOFC anode via compaction pressure control during forming", *Solid State Ionics*, vol. 166, no. 1-2, pp. 13-17.
- Levec, J., Saez, A.E. & Carbonell, R.G. (1986), "Hydrodynamics of trickling flow in packed beds. Part II: experimental observations.", *AIChE Journal*, vol. 32, no. 3, pp. 369-380.
- Mohanty, K.K. 2003, "The near-term energy challenge", *AIChE Journal*, vol. 49, no. 10, pp. 2454-2460.
- Quiblier, J.A. (1984), "New three-dimensional modeling technique for studying porous media", *Journal of Colloid and Interface Science*, vol. 98, no. 1, pp. 84-102.
- Politis, M.G., Kikkinides, E.S., Kainourgiakis, M.E. & Stubos, A.K. (2008), "A hybrid process-based and stochastic reconstruction method of porous media", *Microporous and Mesoporous Materials*, vol. 110, no. 1, pp. 92-99.
- Rintoul, M.D. & Torquato, S. (1997), "Reconstruction of the structure of dispersions", *Journal of Colloid and Interface Science*, vol. 186, no. 2, pp. 467-476.
- Roache, J. (1982), *Computational Fluid Dynamics*, Hermosa Publishing, Albuquerque.
- Sankaran, S. & Zabarar, N. (2006), "A maximum entropy approach for property prediction of random microstructures", *Acta Materialia* vol. 54, pp. 2265-2276.
- Sheehan, N. & Torquato, S. (2001), "Generating microstructures with specified correlation functions", *Journal of Applied Physics*, vol. 89, no. 1, pp. 53-60.
- Spanne, P., Thovert, J.F., Jacquin, C.J., Lindquist, W.B., Jones, K.W. & Adler, P.M. (1994), "Synchrotron computed microtomography of porous media: Topology and transports", *Physical Review Letters*, vol. 73, no. 14, pp. 2001-2004.
- Stubos, A. (1990) *Modeling and Applications of Transport Phenomena in Porous Media*, von Karman Institute for Fluid Dynamics, Lecture Series 1990-01.
- Thovert, J.-., Yousefian, F., Spanne, P., Jacquin, C.G. & Adler, P.M. (2001), "Grain reconstruction of porous media: Application to a low-porosity Fontainebleau sandstone", *Physical Review E*, vol. 63, no. 6 I.
- Tomutsa, L., Silin, D.B. & Radmilovic, V. (2007), "Analysis of chalk petrophysical properties by means of submicron-scale pore imaging and modeling", *SPE Reservoir Evaluation and Engineering*, vol. 10, no. 3, pp. 285-293.

- Torquato, S. (2005), *Microstructure Optimization*, in Handbook of Materials Modeling, Edited by Sidney Yip, Springer-Verlag, New York
- Torquato, S. (2002), *Random Heterogeneous Materials: Microstructure and Macroscopic Properties*, Springer-Verlag, New York.
- Torquato, S. & Lee, S.B. (1990), "Computer simulations of nearest-neighbor distribution function and related quantities for hard-sphere systems", *Physica A*, vol. 167, pp. 361-383.
- Van Kats, F.M. & Egberts, P.J.P. (1998), "Spreading dynamics modeled by lattice-Boltzmann techniques", *Journal of Colloid and Interface Science*, vol. 205, no. 1, pp. 166-177.
- Yeong, C.L.Y. & Torquato, S. (1998a), "Reconstructing random media", *Physical Review E*, vol. 57, no. 1, pp. 495-506.
- Yeong, C.L.Y. & Torquato, S. (1998b), "Reconstructing random media. II. Three-dimensional media from two-dimensional cuts", *Physical Review E*, vol. 58, no. 1, pp. 224-233.

IntechOpen



## **Simulated Annealing**

Edited by Cher Ming Tan

ISBN 978-953-7619-07-7

Hard cover, 420 pages

**Publisher** InTech

**Published online** 01, September, 2008

**Published in print edition** September, 2008

This book provides the readers with the knowledge of Simulated Annealing and its vast applications in the various branches of engineering. We encourage readers to explore the application of Simulated Annealing in their work for the task of optimization.

### **How to reference**

In order to correctly reference this scholarly work, feel free to copy and paste the following:

Maurice, G. Politis, Michael E. Kainourgiakis, Eustathios S. Kikkinides and Athanasios K. Stubos (2008). Application of Simulated Annealing on the Study of Multiphase Systems, Simulated Annealing, Cher Ming Tan (Ed.), ISBN: 978-953-7619-07-7, InTech, Available from:  
[http://www.intechopen.com/books/simulated\\_annealing/application\\_of\\_simulated\\_annealing\\_on\\_the\\_study\\_of\\_multiphase\\_systems](http://www.intechopen.com/books/simulated_annealing/application_of_simulated_annealing_on_the_study_of_multiphase_systems)

**INTECH**  
open science | open minds

### **InTech Europe**

University Campus STeP Ri  
Slavka Krautzeka 83/A  
51000 Rijeka, Croatia  
Phone: +385 (51) 770 447  
Fax: +385 (51) 686 166  
[www.intechopen.com](http://www.intechopen.com)

### **InTech China**

Unit 405, Office Block, Hotel Equatorial Shanghai  
No.65, Yan An Road (West), Shanghai, 200040, China  
中国上海市延安西路65号上海国际贵都大饭店办公楼405单元  
Phone: +86-21-62489820  
Fax: +86-21-62489821

© 2008 The Author(s). Licensee IntechOpen. This chapter is distributed under the terms of the [Creative Commons Attribution-NonCommercial-ShareAlike-3.0 License](https://creativecommons.org/licenses/by-nc-sa/3.0/), which permits use, distribution and reproduction for non-commercial purposes, provided the original is properly cited and derivative works building on this content are distributed under the same license.

IntechOpen

IntechOpen